THE JOURNAL OF BIOLOGICAL CHEMISTRY
Vol. 274, No. 18, Issue of April 30, pp. 12488–12498, 1999
Printed in U.S.A.

Escherichia coli DNA Helicase II Is Active as a Monomer*

(Received for publication, December 16, 1998)

Leah E. Mechanic‡§¶, Mark C. Hall¶‖, and Steven W. Matson‖**

*From the ‡Department of Biochemistry and Biophysics, §Protein Engineering and Molecular Genetics Training Program, ‖Department of Biology, and **Curriculum in Genetics and Molecular Biology, University of North Carolina, Chapel Hill, North Carolina 27599*

Helicases are thought to function as oligomers (generally dimers or hexamers). Here we demonstrate that although *Escherichia coli* DNA helicase II (UvrD) is capable of dimerization as evidenced by a positive interaction in the yeast two-hybrid system, gel filtration chromatography, and equilibrium sedimentation ultracentrifugation (K_d = 3.4 μM), the protein is active *in vivo* and *in vitro* as a monomer. A mutant lacking the C-terminal 40 amino acids (UvrDΔ40C) failed to dimerize and yet was as active as the wild-type protein in ATP hydrolysis and helicase assays. In addition, the *uvrDΔ40C* allele fully complemented the loss of helicase II in both methyl-directed mismatch repair and excision repair of pyrimidine dimers. Biochemical inhibition experiments using wild-type UvrD and inactive UvrD point mutants provided further evidence for a functional monomer. This investigation provides the first direct demonstration of an active monomeric helicase, and a model for DNA unwinding by a monomer is presented.

The first DNA helicase was identified and characterized more than 20 years ago (1, 2). Since then, the biochemical properties and biological functions of many helicases have been firmly established (3–5), and new helicases are continually being discovered and characterized from prokaryotic, eukaryotic, and viral systems. Despite the great attention helicases have received in recent years due to their fundamental importance in DNA and RNA metabolism, many details of the mechanism(s) by which helicases couple the energy derived from nucleoside 5′-triphosphate hydrolysis to the separation of the two strands of duplex nucleic acids are still not known.

Several models for helicase-catalyzed unwinding have been proposed (reviewed in Ref. 5). A common feature of these models is the existence of multiple DNA- or RNA-binding sites within the active enzyme. Multiple binding sites are believed to be essential for processive translocation of the helicase along the nucleic acid. This requirement is thought to be satisfied by an oligomeric enzyme, and in general, helicases have been divided into two oligomeric categories: dimers and hexamers. Whereas the assembly state of several hexameric helicases has been described in detail (6–12), information on dimeric helicases has been mostly limited to studies of the *E. coli* Rep enzyme.

Lohman and colleagues (13–15), using a combination of steady-state and pre-steady-state kinetic studies, have demonstrated that DNA binding induces dimerization of *E. coli* Rep helicase and that dimers are the active form of the enzyme. A model for processive DNA unwinding catalyzed by the Rep helicase has been proposed in which the two subunits of the active dimeric enzyme alternate binding to the double-stranded DNA (dsDNA)[1] region at an unwinding fork to catalyze ATP hydrolysis-dependent strand separation (15). In this rolling model, cycling of the two subunits through a duplex region during processive unwinding is driven by changes in single-stranded (ssDNA) and dsDNA binding affinities. These changes in affinity are allosterically regulated by the state of nucleotide binding of each subunit (recently reviewed in Ref. 5).

DNA helicase II (UvrD), which shares approximately 40% amino acid sequence identity with Rep, performs a variety of functions in *E. coli* including essential roles in methyl-directed mismatch repair (16) and nucleotide excision repair (17, 18). In a previous report, UvrD was shown to form dimers and higher order oligomers in solution, and dimerization was stimulated in the presence of ssDNA (19). It has been proposed that UvrD functions as a dimer and may employ an unwinding mechanism similar to that proposed for Rep (5, 20). This suggestion is based on (i) the extensive sequence similarity between Rep and UvrD, (ii) the abundance of data suggesting dimerization is required for activity of the *E. coli* Rep helicase, (iii) the observation that UvrD forms dimers and higher order oligomers in solution, and (iv) current models for helicase-catalyzed DNA unwinding mechanisms in which the requirement for multiple DNA-binding sites is generally satisfied by multiple subunits in an active enzyme. However, there is currently no direct evidence to indicate that UvrD is functional as a dimer or to favor a rolling model for UvrD-catalyzed unwinding.

During the course of a yeast two-hybrid screen of an *E. coli* genomic library using the *uvrD* gene as bait, we found that UvrD interacts with itself in support of the notion of dimerization. However, a UvrD mutant was constructed that failed to dimerize yet functioned in two DNA repair pathways *in vivo* and was active as a ssDNA-stimulated ATPase and a helicase *in vitro*. This result prompted a thorough biophysical and biochemical analysis of the oligomeric state of UvrD. We conclude that UvrD is active as a monomer, and unwinding mechanisms based on a monomeric helicase are discussed.

EXPERIMENTAL PROCEDURES

Materials

Bacterial Strains and Plasmids—E. coli BL21(DE3) (F^- *ompT* [lon] *hsd*$S_B r_B$-m_B- *gal dcm* λDE3) was from Novagen, Inc. BL21(DE3)Δ*uvrD* and JH137Δ*uvrD* were constructed previously in this laboratory (21). JH137 (K91 *din D1*:: MudI (Ap^r*lac*)) was obtained from P. Model.

Plasmids pET-9d, pET-11d, and pLysS were from Novagen, Inc. M13mp7 ssDNA was prepared as described (22). Construction of plasmids that express UvrD and the various UvrD mutants have been

* This work was supported by National Institutes of Health Grant GM 33476 (to S. W. M.). The costs of publication of this article were defrayed in part by the payment of page charges. This article must therefore be hereby marked "*advertisement*" in accordance with 18 U.S.C. Section 1734 solely to indicate this fact.

¶ Both authors contributed equally to this work.

[1] The abbreviations used are: dsDNA, double-stranded DNA; ssDNA, single-stranded DNA; 2-AP, 2-aminopurine; PCR, polymerase chain reaction; AMP-PNP, adenosine 5′-(β,γ-imido)triphosphate; ATP, adenosine nucleoside 5′ triphosphate; bp, base pair.

described previously (21, 23, 24). To construct a plasmid that expressed UvrDΔ40C, pET11d-UvrD was digested to completion with *Bsi*W1. The 5′ extension was filled in using DNA polymerase I (large fragment) and dNTPs, and the plasmid was ligated with T4 DNA ligase. This caused a +1 frameshift at codon 676, changing 5′-GTACGCCACGCTA-AGTTT-3′ (Val-Arg-His-Ala-Lys-Phe) to 5′-GTACGTACGCCACGCTA-A-3′ (Val-Arg-Thr-Pro-Arg-TER). The *uvrDΔ40C* mutation was confirmed by DNA sequencing using the Sequenase kit (U. S. Biochemical Corp.).

Oligonucleotides, Nucleotides, and Proteins—Oligonucleotide $(dT)_{16}$ was from The Midland Certified Reagent Co. The 2-aminopurine (2-AP)-substituted oligonucleotides were synthesized by Genosys. All nucleotides were from Amersham Pharmacia Biotech. All enzymes used for cloning and PCR were from New England Biolabs, with the exception of T4 DNA ligase, which was from Roche Molecular Biochemicals. Thyroglobulin, catalase, rabbit muscle aldolase, and cytochrome *c* were from Sigma. Human transferrin was from Calbiochem.

Protein Purification—UvrD and UvrDΔ40C were overexpressed prior to purification by growing either a 10-liter culture of BL21(DE3)/pLysS cells containing pET11d-UvrD (21) or BL21(DE3)Δ*uvrD*/pLysS cells containing pET11d-UvrDΔ40C to an optical density (600 nm) of 1.0 at 37 °C. Protein expression was induced by adding 0.4 mM isopropyl-β-D-thiogalactopyranoside, and growth was continued for an additional 4 h. Purification of wild-type helicase II was performed according to a previously published procedure (19). UvrDΔ40C was purified using the same procedure with one modification. UvrDΔ40C was loaded onto an ssDNA-cellulose column (5.8 mg ssDNA/g of cellulose) at 0.1 M NaCl in Buffer A (20 mM Tris-HCl (pH 8.3 at 25 °C), 20% glycerol (v/v), 1 mM EDTA, 0.5 mM EGTA, and 15 mM 2-mercaptoethanol) instead of Buffer A + 0.2 M NaCl. The column was washed using Buffer A + 0.2 M NaCl and eluted using Buffer A + 1 M NaCl.

Methods

Yeast Two-hybrid System—Plasmids and strains for the yeast two-hybrid system were from CLONTECH. An *E. coli* genomic library was constructed previously in pGAD424 (25). The library was screened for UvrD-interacting proteins as described (25). The bait plasmid was pGBT9-UvrD. Vent DNA polymerase was used to amplify the *uvrD* gene by PCR using pET9d-UvrD as target. Amplified *uvrD* was cloned into the *Sma*I site of pGAD424 and pGBT9 to create in-frame translational fusions with the *GAL4* transcriptional activation domain and DNA binding domain, respectively. These constructs were designated pGAD424-UvrD and pGBT9-UvrD.

Deletions from the N and C termini of UvrD were generated using convenient restriction enzyme sites within the *uvrD* gene. The restriction enzymes *Xmn*I, *Ava*II, and *Bst*BI were used to generate the N-terminal deletions *uvrDΔ276N, uvrDΔ309N,* and *uvrDΔ383N,* respectively. The *uvrD* PCR product described in the preceding paragraph was digested individually with each of these enzymes, and the appropriate fragment was purified and ligated into the *Sma*I site of pGAD424 to generate a fusion with the *GAL4* activation domain. Blunt ends were generated by a DNA polymerase I (large fragment)-catalyzed fill-in reaction where necessary. All clones produced in-frame translational fusions and were confirmed by sequence analysis. pGAD424-UvrDΔ40C was generated by digestion of pGAD424-UvrD with *Bsi*WI and *Bgl*II, gel purification, fill-in of the 5′-overhanging ends with DNA polymerase I (large fragment), and re-ligation of the blunt ends.

Two-hybrid interactions were characterized using the *lacZ* reporter gene in strain SFY526 or the *HIS3* reporter gene in strain HF7c. In HF7c, interactions were identified by growth on media lacking histidine. Assays for β-galactosidase activity encoded by the *lacZ* gene in SFY526 were performed using the substrate *o*-nitrophenyl β-D-galactopyranoside as described by the supplier (CLONTECH), and quantified as Miller units (26).

Analytical Ultracentrifugation—Sedimentation equilibrium and sedimentation velocity experiments were done using a Beckman XL-A centrifuge and an An-60ti rotor at 20 °C. Protein was prepared for these experiments by extensive dialysis into the appropriate buffer. For sedimentation equilibrium experiments the buffer contained 20 mM Tris-HCl (pH 8.3 at 25 °C), 0.2 M NaCl, 20% glycerol (v/v), 1 mM EDTA, 1 mM EGTA, and 15 mM 2-mercaptoethanol. For velocity sedimentation experiments the buffer contained 25 mM Tris-HCl (pH 7.5 at 25 °C), 50 mM NaCl, 3 mM $MgCl_2$, 20% glycerol (v/v), and 5 mM 2-mercaptoethanol. Solvent densities (ρ) were measured using a Mettler DA-110 M density meter. The partial specific volume for UvrD and UvrDΔ40C was calculated to be $\nu = 0.729$ at 20 °C using SEDNTERP (27).

Equilibrium ultracentrifugation experiments were performed in 6-channel (1.2 cm path) charcoal-epon centrifuge cells (Beckman). The equilibrium experiment was performed using three different concentrations of UvrD (1.1, 2.1, and 3.8 μM) and UvrDΔ40C (2.8, 5.0, and 8.4 μM). Protein concentrations were determined from absorbances collected during the low speed scans in the ultracentrifuge. Scans at 280 nm were recorded every 2 h. After 30 h the cell was judged to be at equilibrium. This was confirmed by subtracting successive plots and examining residuals for the absence of any systematic patterns. For UvrD the speeds used were 5,000, 7,500, and 10,000 rpm, and for UvrDΔ40C the speeds were 7,200, 8,600, and 12,600 rpm. All concentrations of UvrDΔ40C reached equilibrium within the 30-h period for each speed. Three of the data sets obtained with the wild-type protein did not reach equilibrium during the course of the experiment (1.1 μM at 5,000 rpm, 2.1 μM at 5,000 rpm, and 3.8 μM at 10,000 rpm) and were not considered in the analysis.

Several models were fit to data from equilibrium centrifugation experiments using NONLIN (28). Separate concentrations and different speeds were analyzed individually, in groups, and globally. The models primarily considered were single ideal species and ideal monomer ↔ dimer equilibrium. In addition, other models were examined including non-ideality, monomer ↔ trimer and monomer ↔ tetramer. Molecular masses were calculated based on the values for σ (reduced molecular mass) (see Equation 1) according to methods described (28).

$$\sigma = \frac{M(1 - \nu\rho)\omega^2}{RT} \qquad \text{(Eq. 1)}$$

M is the molecular weight; R is the gas constant; T is the temperature in degrees Kelvin; ν is the partial specific volume (ml/g) of the protein; ω is the angular velocity of the rotor (radians/s), and ρ is the measured density of the buffer (g/ml). K_d values were calculated using Equation 2 for the model of monomer ↔ dimer equilibrium (see Equation 3).

$$C(r) = \delta + C_{1,0}e^{(\sigma_1\xi)} + C_{1,0}{}^2e^{(\ln K_2 + 2\sigma_1\xi)} \qquad \text{(Eq. 2)}$$

$$\xi = (r^2 - r_0{}^2)/2 \qquad \text{(Eq. 3)}$$

$C(r)$ is the total protein concentration (mg/ml) at the radius (r); δ is the base-line offset used to compensate for absorbance measurements of 0 not being precisely equal to 0 protein concentration; $C_{1,0}$ is the monomer concentration at the reference distance (r_0); and K_2 is the association constant for monomer ↔ dimer model (28, 29). The reference distance, or reference radial position, is chosen in data analysis and is usually near the meniscus in the cell. σ_1 is the reduced molecular weight for the monomer.

Velocity experiments were performed with 350-μl samples in two-channel charcoal epon centerpieces (1.2 cm path) (Beckman). The rotor speed was 50,000 rpm. Initial protein concentrations were approximately 7.5 μM. Experimental samples analyzed in the presence of nucleotide contained 0.2 mM AMP-PNP. For reactions containing ssDNA, the DNA molecule used was a $(dT)_{16}$ oligonucleotide containing the modified base 2-aminopurine (AP). The two ssDNA substrates were either 5′-TTTTT(AP)TTTT(AP)TTTTT-3′ or 5′-TTT(AP)TT(AP)TT(AP)TT(AP)TTT-3′. The molar ratio of protein to DNA was 1:1.25. Data obtained from sedimentation velocity experiments in the absence of DNA (protein alone or protein with nucleotide) were collected at either 285 or 290 nm. In the presence of DNA, sedimentation was monitored at 315 nm to detect only the modified $(dT)_{16}$ molecule. Scans were recorded at 1-min intervals in a continuous mode.

Sedimentation velocity data were analyzed using the program Svedberg (30). Sedimentation coefficients (s^*) were determined by fitting the modified Fujita-MacCoshman equation for a single species and two species to the data (31). For experiments containing DNA, the program dCdT (32) was used to obtain s_w values for interacting species. The s_w values obtained using dCdT were consistent with s^* values obtained using Svedberg. A control sedimentation velocity experiment performed using the 2-AP oligonucleotide in the absence of protein confirmed the identity of the two species in the experiment containing DNA (DNA alone and DNA-protein complex). The values s^* and s_w were corrected for solvent density and viscosity and normalized to standard conditions to produce the $s_{20,w}$ value (33, 34). Values for ν were corrected for percentage glycerol as described (35, 36).

Gel Filtration—The apparent molecular mass of UvrD and UvrD mutants was determined in the presence and absence of ligands using a Superose 12 HR 10/30 column (Amersham Pharmacia Biotech) and high pressure liquid chromatography system (Rainin, model HPXL) at 4 °C. Column buffer was 25 mM Tris-HCl (pH 7.5), 100 mM NaCl, 3 mM $MgCl_2$, 5 mM 2-mercaptoethanol, and 20% glycerol. When present in the

column buffer, ATP was 0.5 mM. Proteins (25 μg) were injected onto the column in a volume of 50 μl at a flow rate of 0.2 ml/min. When present, ^{32}P-labeled oligonucleotide $(dT)_{16}$ was included in the loaded sample at a concentration of 11.2 μM. Samples were passed through the column at a flow rate of 0.2 ml/min, and elution of protein peaks was monitored continuously by absorbance at 280 nm. The elution of $(dT)_{16}$ was followed by scintillation counting of column fractions. Samples were subjected to centrifugation prior to loading to remove particulate matter and any insoluble protein. Comparison of protein concentration measurements made before and after application to the column revealed that essentially all protein was soluble and recovered in a single peak. A standard curve of log molecular mass *versus* retention time was generated in the absence of ATP using the following proteins under the column buffer conditions described above: thyroglobulin (668,000 Da), catalase (212,000 Da), rabbit muscle aldolase (158,000 Da), human transferrin (80,000 Da), and cytochrome *c* (12,400 Da). The retention time of all protein standards was not significantly altered by the presence of ATP.

Genetic Assays—Genetic complementation assays were performed using JH137 and derivatives. UV irradiation survival assays (23) and determination of spontaneous mutation frequencies (37) were performed as described previously.

ATPase Assays—The standard ATPase reaction mixture contained 25 mM Tris-HCl (pH 7.5), 3 mM $MgCl_2$, 20 mM NaCl, and 5 mM 2-mercaptoethanol. The reaction stop solution was 33 mM EDTA, 7 mM ATP, and 7 mM ADP. In general, reactions were executed and products separated by thin layer chromatography as described previously (38). All reactions were incubated at 37 °C. When [^{3}H]ATP was used, the results were quantified using a liquid scintillation counter. When [α-^{32}P]ATP was used, the results were quantified using a Storm 840 PhosphorImager and ImageQuant software (Molecular Dynamics). Background signals measured in the absence of enzyme were typically between 1 and 2% and were subtracted from the experimental data.

For inhibition assays the concentration of UvrD was 4 nM and the concentrations of UvrD-K35M, UvrD-E221Q, and UvrD-R605A were 125 nM. Reaction mixtures (30 μl) contained 1 mM [α-^{32}P]ATP and 1.8 μM oligonucleotide $(dT)_{16}$ (molecules). Wild-type and mutant helicase II enzymes were mixed together at 15 times their final concentrations and preincubated on ice for 10 min. Reactions were initiated by adding enzyme (wild-type, mutant, or a mixture of both) to reaction mixtures at 37 °C. Samples (5 μl) were removed at 1-min intervals (within the linear range of the reaction) and quenched with 5 μl of stop solution.

Reactions for examining the protein concentration dependence of the UvrD-catalyzed ATPase reaction were identical to those for the inhibition assays except that the UvrD concentration was varied from 1 to 64 nM, and bovine serum albumin was included at 50 μg/ml. As the UvrD concentration was decreased, samples were removed at increasing time intervals to ensure production of a detectable signal. All data points fell within the linear range of the reaction.

To compare the k_{cat} values of UvrD and UvrDΔ40C, reaction mixtures (30 μl) contained 0.8 mM [^{3}H]ATP and 30 μM M13mp7 ssDNA (nucleotide phosphate). Reactions were initiated with enzyme at a final concentration of 2 nM. Samples (8 μl) were removed and quenched with 8 μl of stop solution at 2-min intervals. To compare K_m values of UvrD and UvrDΔ40C, reaction mixtures (20 μl) contained 2 nM enzyme, 30 μM M13mp7 ssDNA (nucleotide phosphate), and increasing concentrations (25–500 μM) of [α-^{32}P]ATP. Reactions were initiated with [α-^{32}P]ATP and incubated for 10 min. Duplicate samples of 5 μl were removed and quenched with 5 μl of stop solution.

Helicase Assays—Helicase reaction mixtures (20 μl) contained 25 mM Tris-HCl (pH 7.5), 3 mM $MgCl_2$, 20 mM NaCl, 5 mM 2-mercaptoethanol, and 3 mM ATP. For inhibition experiments, the reaction mixtures also included 0.5 μM 20-mer oligonucleotide molecules and 5 nM 20-bp partial duplex [^{32}P]DNA substrate molecules. The partial duplex substrate was prepared as described previously (23). The unlabeled 20-mer was the same sequence as the ^{32}P-labeled 20-mer used to make the partial duplex substrate and was included at molar excess to prevent reannealing of unwound ^{32}P-labeled 20-mer. The concentration of UvrD was 1 nM, and the concentrations of UvrD-K35M, UvrD-E221Q, and UvrD-R605A were 3 nM. Wild-type and mutant helicase II enzymes were mixed together at 10 times their final concentrations and incubated on ice for 10 min. Subsequently, enzymes were incubated on ice with the partial duplex DNA substrate in the reaction buffer for 5 min prior to initiation of the reactions. Reactions were initiated by adding ATP and unlabeled 20-mer at 37 °C. After incubation at 37 °C for 3 min, reactions were quenched with 10 μl of stop solution (37.5% glycerol, 50 mM EDTA, 0.05% each of xylene cyanol and bromphenol blue, and 0.3% SDS).

For the biochemical comparison of UvrD- and UvrDΔ40C-catalyzed unwinding reactions, the standard reaction mixtures included approximately 0.2 nM 92-bp partial duplex [^{32}P]DNA substrate molecules prepared as described previously (23). Reactions were initiated with the indicated concentration of enzyme at 37 °C, incubated for 10 min, and quenched with 10 μl of stop solution. All reaction products were resolved on 8% non-denaturing polyacrylamide gels (20:1 cross-linking ratio), and the results were visualized and quantified using a Storm 840 PhosphorImager and ImageQuant software (Molecular Dynamics).

RESULTS

UvrD Interacts with Itself in the Yeast Two-hybrid System—The formation of dimers and higher order oligomers by UvrD has been suggested based on gel filtration techniques and glutaraldehyde cross-linking (19). This observation is consistent with the idea that the active form of UvrD may be dimeric, as has been demonstrated for Rep helicase (13–15). We discovered independent evidence for UvrD dimerization that enabled us to begin to identify the domain(s) responsible for this phenomenon.

In a yeast two-hybrid screen to identify proteins that interact with UvrD, an interacting clone was isolated that was identical to a portion of the *uvrD* gene. This interacting clone encoded a region of UvrD lacking the N-terminal 244 amino acids, suggesting that the N terminus of helicase II was not essential for oligomerization. Subsequently, an interaction between two full-length UvrD proteins was demonstrated (Fig. 1*A*). To define further the interaction domain, various deletion mutants were constructed and analyzed for their ability to interact with wild-type UvrD in the yeast two-hybrid system using assays for β-galactosidase activity to quantify interaction-dependent expression of a *lacZ* reporter gene (Fig. 1*B*). The results indicated that the C-terminal half of UvrD was sufficient to produce a detectable interaction. Removal of 383 amino acids from the N terminus or 40 amino acids from the C terminus abolished the two-hybrid interaction. The latter result was particularly interesting because the UvrDΔ40C mutant had been partially characterized previously and found to be indistinguishable from wild-type UvrD.[2] The two-hybrid data suggest that UvrDΔ40C has a defect in oligomerization, which prompted a careful examination of this property using both UvrD and UvrDΔ40C. The existence of a mutant that fails to dimerize, yet has wild-type biochemical activity, has significant implications for the UvrD-unwinding mechanism.

Assembly State of UvrD and UvrDΔ40C—The assembly state (*i.e.* monomer, dimer, oligomer) of UvrD and UvrDΔ40C was examined by analytical sedimentation equilibrium ultracentrifugation experiments (Fig. 2). The predicted molecular masses, based on amino acid composition, are 82,151 Da for UvrD and 77,850 Da for UvrDΔ40C. The average apparent molecular mass, as revealed by equilibrium sedimentation, was 119.8 kDa for UvrD and 61.1 kDa for UvrDΔ40C. These apparent molecular masses represent the average mass of species present in the ultracentrifuge cell.

For wild-type helicase II, molecular mass was consistent with a mixture of monomers and dimers. Several models were fit to the equilibrium centrifugation data for UvrD and UvrDΔ40C, including single ideal species, monomer ↔ dimer, monomer ↔ trimer, monomer ↔ tetramer, and non-ideality. All of the data analyzed for UvrD were most consistent with the monomer ↔ dimer model described by Equation 2 (Fig. 2*A, solid line*). Using this equation, the K_d for dimerization was calculated to be 3.4 μM.

The average apparent molecular mass determined for UvrDΔ40C was consistent with the monomeric molecular mass. In addition, the apparent molecular mass of UvrDΔ40C did not increase with an increase in protein concentration, even

[2] L. E. Mechanic and S. W. Matson, unpublished data.

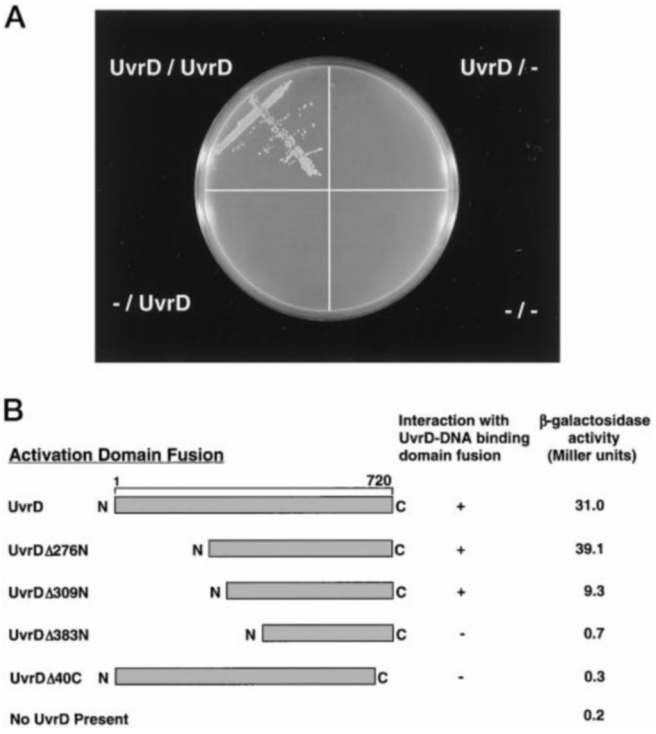

FIG. 1. **UvrD interacts with itself in the yeast two-hybrid system.** *A,* HF7c cells containing pGAD424 and pGBT9 with or without the *uvrD* gene were grown at 30 °C on complete synthetic media lacking tryptophan, leucine, and histidine and supplemented with 1 mM 3-amino-1,2,4-triazole. Each quadrant contains cells streaked from a single transformant that was colony-purified. Labels represent fusion proteins present in the HF7c cells in the order, DNA binding domain fusion/transcriptional activation domain fusion. A − represents the absence of *uvrD* from the fusion construct. *B,* β-galactosidase activity was measured in yeast SFY526 cells using *o*-nitrophenyl β-D-galactopyranoside as described under "Experimental Procedures." Truncations of the *uvrD* gene were constructed in pGAD424 and were tested for an interaction in the presence of pGBT9-UvrD. A + indicates the presence of an interaction and a − indicates the absence of an interaction. All assays scored as interactions displayed at least a 40-fold increase in β-galactosidase activity (Miller units) compared with a control in the absence of a UvrD-activation domain fusion. All results represent the average of 2 or 3 separate experiments using independent transformants.

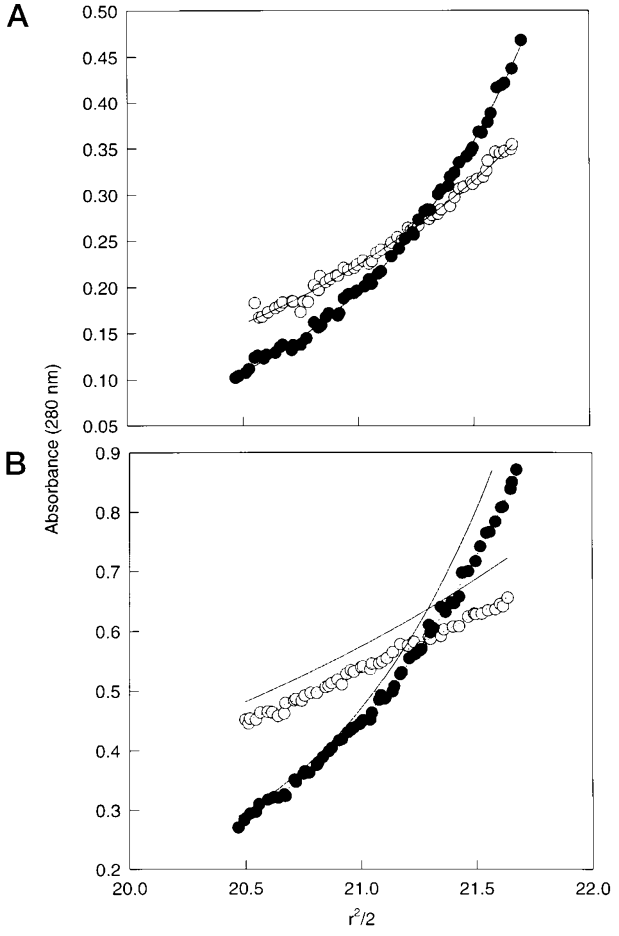

FIG. 2. **Sedimentation equilibrium of UvrD and UvrDΔ40C.** The association state of UvrD and UvrDΔ40C was analyzed using analytical ultracentrifugation. Data shown are a subset of all the data acquired at three different speeds and protein concentrations for both UvrD and UvrDΔ40C as described under "Experimental Procedures." *A,* UvrD samples (2.1 μM) were sedimented at 7,500 rpm (○) and 10,000 rpm (●). The equation for the monomer ↔ dimer equilibrium (2) was fit to the data (*solid line*). *B,* UvrDΔ40C (5.0 μM) samples were sedimented at 7200 (○) and 12,960 rpm (●). The monomer ↔ dimer model, using Equation 2 (*solid line*) and the equation for a single ideal species, $C(r) = \delta + C_{1,0}e^{(\sigma_1\xi)}$ (*dashed line*) (28), were fit to the data. Protein absorbance was measured at 280 nm. Data analysis was performed using NONLIN (28) as detailed under "Experimental Procedures."

at protein concentrations more than 2-fold greater than the highest wild-type protein concentration. The lower than expected apparent molecular mass for UvrDΔ40C may be due to the presence of 20% glycerol in the ultracentrifuge cell. It has been reported that glycerol can affect the observed molecular mass in equilibrium sedimentation experiments (36). If this is the case, then the molecular mass reported for UvrD may be an underestimate. All of the data for UvrDΔ40C were most consistent with a model for a single-ideal species (Fig. 2*B, dashed line*) with a monomeric molecular mass. A dimerization constant for UvrDΔ40C could not be determined since the monomer ↔ dimer model failed to converge to the data (Fig. 2*B, solid line*). Thus, UvrDΔ40C fails to dimerize, consistent with the results obtained from the yeast two-hybrid system.

To determine whether ligands could enhance the dimerization of either protein, sedimentation velocity experiments were performed in the presence and absence of a poorly hydrolyzable ATP analog and ssDNA. It has been shown previously, using other techniques, that dimerization of Rep occurs only on ssDNA and is therefore ligand-induced (13, 15). It is important to note that the sedimentation coefficient ($s_{20,w}$) reflects both the size and shape of the protein. The $s_{20,w}$ of a dimer should increase by a factor of 1.5 over that for a monomer (39, 40). Such an increase has been demonstrated previously for the gene 41 helicase from phage T4 which dimerizes in the presence of GTP (11). Sedimentation velocity experiments with UvrD were possible only in the presence of DNA and AMP-PNP, due to the limited solubility of wild-type helicase II in the absence of DNA (Table I). However, it was possible to measure sedimentation velocity for UvrDΔ40C in the absence of ligands, in the presence of nucleotide, and in the presence of DNA plus nucleotide.

The UvrDΔ40C sedimentation coefficient in the absence of ligands was 7.0 ± 0.3 (Table I). Scans of the ultracentrifuge cell during the course of the velocity sedimentation experiments failed to show any biphasic character suggestive of multiple species in the cell (*i.e.* populations of monomers and dimers). Moreover, multiple species models did not fit the data as well as the modified Fujita-MacCoshman function for a single species. The sedimentation coefficient for UvrDΔ40C decreased in the presence of an ATP analog (AMP-PNP) relative to that of the protein alone and decreased further in the presence of $(dT)_{16}$ and AMP-PNP. The decrease in $s_{20,w}$ indicates that the protein is undergoing a conformational change in the presence of these ligands. The change in $s_{20,w}$ is not consistent with the notion that the protein dimerizes in the presence of either one

TABLE I
Sedimentation coefficients

Velocity sedimentation experiments were performed as described under "Experimental Procedures." UvrD and UvrDΔ40C were approximately 7.5 μM. Data from experiments containing protein alone and those with protein and AMP-PNP (0.2 mM) were collected at 290 nm. Data from experiments containing the 2-AP-modified $(dT)_{16}$ oligonucleotide were collected at 315 nm. DNA to protein molar ratios were 1.25:1. s^* values for the protein alone and protein plus AMP-PNP were obtained using Svedberg (30). Experiments containing DNA were analyzed using the dCdT program, and s_w values were obtained based on the assumption of interacting species (32). s^* and s_w (uncorrected sedimentation coefficients) were normalized to standard conditions ($s_{20,w}$) as described under "Experimental Procedures."

Enzyme	Ligand	$s_{20,w}$ (S)
UvrDΔ40C		7.0 ± 0.3
	AMP-PNP	5.7 ± 0.3
	AMP-PNP, $(dT)_{16}$	4.8 ± 0.1
UvrD	AMP-PNP, $(dT)_{16}$	5.1 ± 0.1

or both ligands. Even if the assumption that this protein behaves as an anhydrous sphere is incorrect, it is unlikely that the sedimentation coefficient would decrease upon dimerization because $s_{20,w}$ is directly proportional to the molecular mass of the species and inversely proportional to shape factors. The sedimentation coefficient for wild-type helicase II in the presence of AMP-PNP and DNA was 5.1 ± 0.1. This was strikingly similar to the result obtained for UvrDΔ40C under the same conditions. It is known from the equilibrium sedimentation experiments described above that UvrDΔ40C behaves as a monomer. Thus, this result suggests that the monomeric form of wild-type UvrD may be stabilized in the presence of an ATP analog and ssDNA.

UvrDΔ40C Elutes as a Monomer on a Gel Filtration Column—To confirm the UvrDΔ40C oligomerization defect revealed in the yeast two-hybrid and ultracentrifugation experiments, high pressure liquid chromatography gel filtration was used to determine the apparent molecular mass of UvrD and UvrDΔ40C in the presence and absence of ligands. In the absence of ligands, UvrD eluted as a single peak with an apparent molecular mass between that expected for a monomeric (82 kDa) and dimeric (164 kDa) protein (Fig. 3*A* and Table II). Under very similar solution conditions (specifically the presence of Mg^{2+}) Runyon *et al.* (19) observed the same result, and it is consistent with a rapid equilibrium between monomeric and oligomeric species. In contrast to UvrD, UvrDΔ40C eluted as a single peak consistent with the predicted molecular mass for the monomeric protein (78 kDa). It should also be noted that the UvrD elution peak was consistently broader than that of UvrDΔ40C and exhibited a shallow trailing slope, suggesting that UvrD existed as a heterogeneous population of molecules (Fig. 3, *A* and *B*). The symmetry of the UvrDΔ40C peak is consistent with a homogeneous population of molecules.

In the presence of ATP, UvrD eluted with a lower apparent molecular mass than in the absence of ATP (Fig. 3*B* and Table II) but still appeared to exist in a rapid equilibrium between monomeric and dimeric species. The apparent molecular mass of UvrDΔ40C did not change significantly in the presence of ATP, again suggesting that this protein exists in solution as a monomer. The shift in the UvrD elution peak is consistent with the notion that ATP binding stabilizes the monomeric form of UvrD. The shift to a lower apparent molecular mass is not consistent with an ATP-induced dimerization of UvrD.

To investigate the possibility that DNA binding affects the oligomeric state of UvrD or restores the ability of UvrDΔ40C to dimerize, gel filtration was performed using a pre-formed enzyme-ssDNA complex. In the presence of ATP and oligonucleotide $(dT)_{16}$, the apparent molecular masses of UvrD and UvrDΔ40C increased by approximately the same amount compared with experiments in which only ATP was present (Table II, 119 *versus* 98 kDa for UvrD and 91 *versus* 73 kDa for

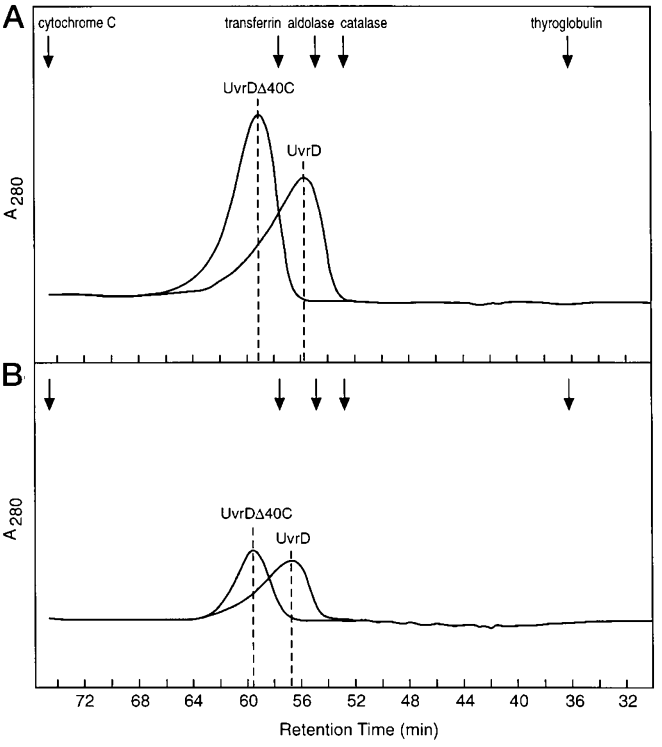

FIG. 3. **UvrD and UvrDΔ40C elute from a Superose 12 column at different positions.** 25 μg of UvrD or UvrDΔ40C were applied to a Superose 12 column as described under "Experimental Procedures" in the absence (*A*) and presence (*B*) of 500 μM ATP. The retention times of the samples were defined as the points of maximum absorbance at 280 nm on the elution traces and are indicated by the *vertical dashed lines*. Independent traces of UvrD and UvrDΔ40C were superimposed on one another. *Arrows* indicate the elution peaks of the five proteins used to generate the standard curve for apparent molecular mass calculations. *B,* the absorbance at 280 nm was initially normalized to zero to eliminate the contribution of ATP to the signal. This resulted in the lower apparent absorbances of UvrD and UvrDΔ40C compared with those in *A*.

TABLE II
Gel filtration of UvrD and UvrD mutants

Sample[a]	Retention time[b]	Apparent molecular mass[c]
	min	*kDa*
UvrD	55.7, 55.8	109
UvrDΔ40C	59.2, 60.0	71
UvrD-K35M	55.9	107
UvrD-E221Q	55.2	116
UvrD-R605A	56.8	97
UvrD (+ATP)[d]	56.6, 56.8	98
UvrDΔ40C (+ATP)[d]	59.3, 59.4	73
UvrD (+ATP, +$(dT)_{16}$)[e]	54.9, 55.0	119
UvrDΔ40C (+ATP, +$(dT)_{16}$)[e]	57.4, 57.4	91
$(dT)_{16}$[c]	68.6	26

[a] 25 μg of each protein were loaded in a volume of 50 μl (final concentration = 6 μM).
[b] Retention times of duplicate trials are shown to demonstrate reproducibility of results.
[c] Results obtained with UvrD and UvrDΔ40C represent the average of two identical experiments. Results obtained with UvrD point mutants represent a single trial. Apparent molecular mass was determined using a standard curve as described under "Experimental Procedures."
[d] 0.5 mM ATP was included in the sample and in the column buffer.
[e] ^{32}P-Labeled $(dT)_{16}$ was included in the sample at a concentration of 11.2 μM.

UvrDΔ40C). Since $(dT)_{16}$ eluted from the column with an apparent molecular mass of 26 kDa (Table II), the size of the increase in each case was consistent with that expected from binding of $(dT)_{16}$ to the enzyme and was not large enough to suggest a stimulation of oligomerization. It is important to note that the apparent molecular mass of the UvrDΔ40C-$(dT)_{16}$ complex was still significantly lower than that of the UvrD-$(dT)_{16}$ complex. Thus, the oligomerization defect exhibited by UvrDΔ40C in the absence of DNA was not corrected by the presence of ssDNA. We confirmed that the protein-$(dT)_{16}$ complex was reasonably stable during the gel filtration experiments by using radiolabeled $(dT)_{16}$ and comparing the elution positions of the DNA and protein (data not shown). Although the protein-ssDNA complexes were clearly in a rapid equilibrium between bound and unbound states relative to the time course of the experiments, the concentration of $(dT)_{16}$ in the protein peak indicated that greater than 60% of the helicase II was bound to DNA.

Genetic and Biochemical Characterization of UvrDΔ40C—Since UvrDΔ40C fails to oligomerize, and oligomerization has been suggested to be essential for helicase activity (5), it was of interest to evaluate the activity of UvrDΔ40C in genetic and biochemical assays. The ability of UvrDΔ40C to complement the loss of UvrD in methyl-directed mismatch repair and excision repair was examined using a strain lacking the *uvrD* gene. JH137Δ*uvrD* was transformed with pET9d-UvrDΔ40C and pET9d-UvrD. Uninduced expression of UvrD and UvrDΔ40C from these constructs in JH137Δ*uvrD* was detectable by Western blot and was similar to chromosomal levels of expression of the wild-type gene in JH137 (data not shown). To assess function in methyl-directed mismatch repair, the spontaneous mutant frequency was measured by quantifying the number of spontaneously arising rifampicin-resistant colonies. Previous studies have shown that wild-type UvrD, expressed from a plasmid, fully complements the loss of helicase II (23, 37, 41). The relative mutability of JH137Δ*uvrD* was 240-fold greater than the parental strain, JH137 (data not shown). JH137 Δ*uvrD* containing pET9d-UvrD or pET9d-UvrDΔ40C exhibited relative mutant frequencies of 1.01 and 0.92, respectively, demonstrating complete complementation of the *uvrD* deletion (Table III). The UV sensitivity of these strains was also measured at increasing doses of UV irradiation to evaluate nucleotide excision repair function. The UV sensitivity of JH137Δ*uvrD*/pET9d-UvrDΔ40C was comparable to that of JH137 and JH137Δ*uvrD*/pET9d-UvrD (data not shown). Thus, UvrDΔ40C is fully functional in both mismatch and excision repair.

UvrDΔ40C was also characterized in biochemical assays. UvrD and UvrDΔ40C were purified to apparent homogeneity (data not shown), and UvrDΔ40C was assayed for ssDNA-stimulated ATPase activity and DNA helicase activity. The ssDNA binding ability of UvrDΔ40C was investigated previously and was found to be similar to that of the wild-type protein.[2] The turnover rates for ssDNA-stimulated ATP hydrolysis (k_{cat}) for both proteins were not significantly different (147 *versus* 157 s^{-1}). In addition, both UvrDΔ40C and UvrD appeared to interact with nucleotide with the same affinity as evidenced by the nearly identical K_m values for ATP (62 *versus* 50 μM). The helicase reaction catalyzed by each protein was measured using a 92-bp partial duplex DNA substrate (Fig. 4). UvrD and UvrDΔ40C unwound the partial duplex substrate with equivalent efficiency. Similar results were obtained with a 238-bp blunt duplex substrate (data not shown). The rates of unwinding of the 92-bp partial duplex substrate by UvrD and UvrDΔ40C during the course of a 10-min reaction were similar. In fact, the rate of unwinding catalyzed by UvrDΔ40C was reproducibly slightly greater than that of UvrD (data not shown). Thus, UvrDΔ40C possesses wild-type ATPase and helicase activities *in vitro*, consistent with its ability to function *in vivo*.

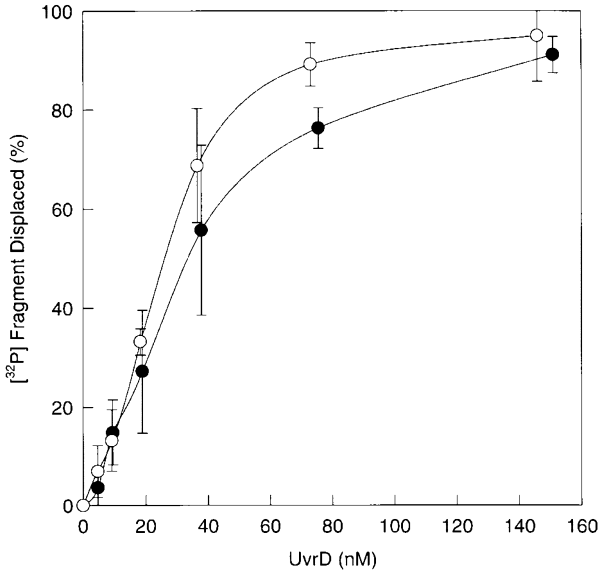

FIG. 4. **Helicase activity of UvrD and UvrDΔ40C.** The unwinding activity of UvrD (●) and UvrDΔ40C (○) was measured using a 92-bp partial duplex substrate as described under "Experimental Procedures." The fraction of unwound substrate molecules was calculated for each protein concentration as outlined (24). Data represent the average of at least 3 independent experiments, and *error bars* are standard deviations about the mean. *Continuous lines* connecting data points were drawn using a cubic spline algorithm (SigmaPlot).

The ssDNA-stimulated ATPase Activity of UvrD Is Independent of Protein Concentration—Since UvrDΔ40C fails to oligomerize and exhibits wild-type biochemical and genetic activity, we suggest that the protein is functional as a monomer. This prompted further investigations to determine if wild-type UvrD was also functional as a monomer. Toward this end, several biochemical properties of UvrD were evaluated.

The k_{cat} for ssDNA-stimulated ATP hydrolysis catalyzed by UvrD was previously reported to increase by a factor of 2.5 as a function of enzyme concentration between 2 and 10 nM (19). Thus, the rate of hydrolysis of UvrD was non-linearly dependent on enzyme concentration in this range. This result was interpreted as evidence for the dimerization of UvrD causing a stimulation of its ATPase activity and as support for an unwinding model involving an active dimeric enzyme. Because the stimulation of ATPase activity was small (only 2.5-fold) and UvrD still demonstrated significant activity at concentrations below the inflection point, we attempted to reproduce this result. Under our reaction conditions, the ssDNA-stimulated ATPase activity of UvrD was independent of protein concentration between 1 and 64 nM. In other words, the rate of ATP hydrolysis was linearly dependent on UvrD concentration (Fig. 5) and provided no evidence for a change in assembly state. Since typical biochemical DNA unwinding assays of UvrD are performed within this range of protein concentrations, these results must be representative of the active species. Unless UvrD has a dimerization constant below 1 nM under these conditions (which we have demonstrated is not the case), these results strongly argue that UvrD monomers are an active form of the enzyme, at least as an ATPase.

ATPase- and Helicase-deficient UvrD Mutants Do Not Inhibit the ssDNA-stimulated ATPase or ATP-dependent Helicase Activities of Wild-type UvrD—As a further test of our conclusion that UvrD monomers are active as DNA helicases, the effect of adding non-functional UvrD mutants to ATPase and helicase

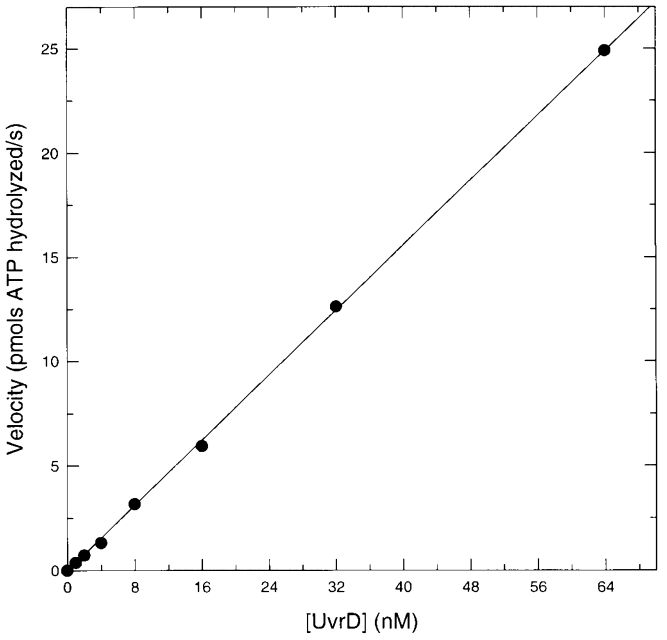

FIG. 5. **The UvrD-catalyzed ssDNA-stimulated ATPase reaction is linearly dependent on enzyme concentration between 1 and 64 nM.** ATPase assays were performed at 37 °C as described under "Experimental Procedures" using oligonucleotide $(dT)_{16}$ as the ssDNA effector. The *straight line* is a linear regression (SigmaPlot) and corresponds to a k_{cat} of 78 s^{-1}. The data for each enzyme concentration were determined in individual experiments involving 5 time points, and each data point represents the average of 2 separate trials.

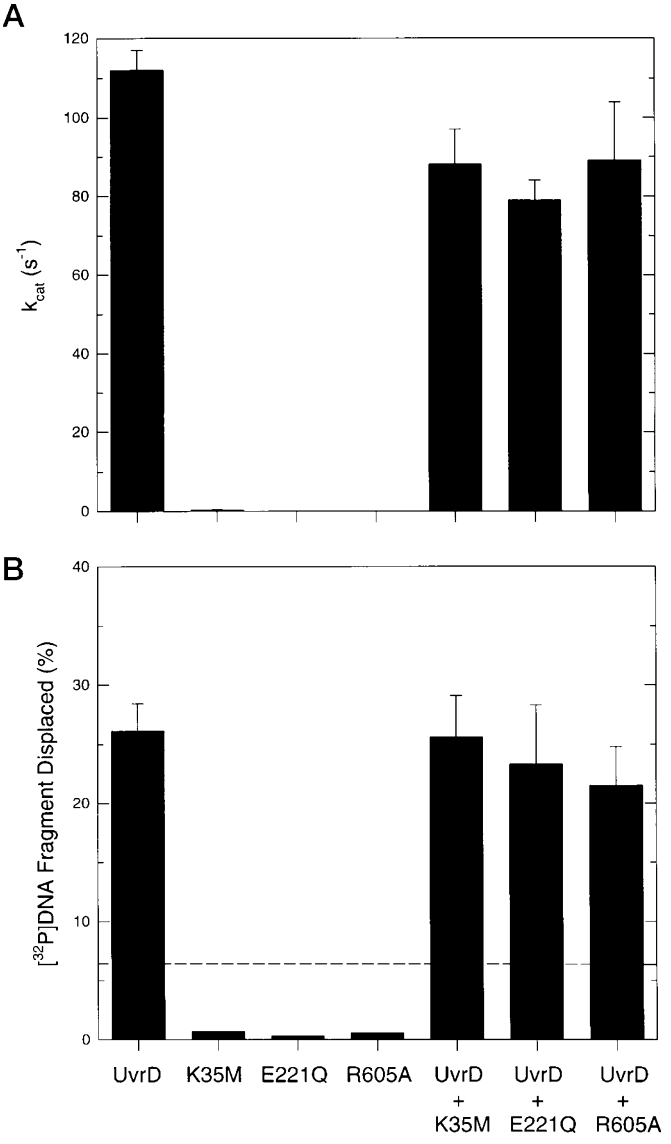

FIG. 6. **Inactive UvrD point mutants do not inhibit the ATPase or helicase activities of wild-type UvrD.** *A,* ATPase assays were performed as described under "Experimental Procedures." When present, the concentration of UvrD was 4 nM, and the concentration of each mutant was 125 nM. Data represent the average of at least 3 independent trials. When both wild-type and mutant enzymes were present, the contribution of mutant enzymes to k_{cat} was subtracted from the data. *B,* helicase assays were performed as described under "Experimental Procedures." When present, the concentration of UvrD was 1 nM, and the concentration of mutant enzymes was 3 nM. The concentration of 20-bp partial duplex DNA substrate molecules in all reactions was 5 nM. The data for wild-type or mutant enzymes alone are an average of at least 3 independent trials. The data for reactions containing both wild-type and mutant enzymes are an average of at least 5 independent trials. The *horizontal dashed line* represents the expected level of unwinding in reactions containing wild-type and mutant enzymes if a dimer were the active species and assuming random association of protein molecules. In both panels *error bars* are standard deviations.

reactions was evaluated. If a dimeric enzyme were required for biochemical activity, then the presence of an excess molar concentration of an inactive mutant should inhibit the reaction catalyzed by the wild-type enzyme, assuming random association of wild-type and mutant subunits. Such a result has been observed previously with the *E. coli* Rep helicase (42) and the bacteriophage T7 gene 4 helicase-primase (43, 44) which are known to function as a dimer and hexamer, respectively. The ssDNA-stimulated ATPase reaction catalyzed by UvrD was measured in the presence of three UvrD point mutants that were severely compromised for ATPase activity (Fig. 6*A*). Each mutant contained a single amino acid substitution of a highly conserved residue within one of the helicase motifs and had been characterized previously (21, 23, 24). Mutant enzymes were present at a 30-fold molar excess over wild-type UvrD, and oligonucleotide $(dT)_{16}$ was used as the ssDNA effector at a molar excess over enzyme to ensure that ssDNA availability was not limiting. Wild-type and mutant enzymes were co-incubated under conditions that favor monomeric species prior to initiation of the reactions to ensure random mixing of protein molecules. At this molar excess of mutant protein, essentially all wild-type molecules should be complexed as a heterodimer with an inactive mutant if dimers are formed. The results clearly demonstrate that the presence of a molar excess of mutant enzyme did not significantly inhibit the ssDNA-stimulated ATPase activity of wild-type UvrD. Although the k_{cat} for ATP hydrolysis appeared to decrease slightly in the presence of each mutant (112 *versus* 79–89 s^{-1}), a requirement for active dimers should have resulted in more dramatic inhibition (to mutant k_{cat} levels 0.058–0.283 s^{-1}). Co-incubation of mutant and wild-type enzymes for a much longer period prior to the reaction did not alter the results (data not shown). In addition, co-incubation of the two proteins in the presence of Mg^{2+} or Mg^{2+}-ATP or inclusion of mutant enzyme at a 300-fold molar excess did not yield different results (data not shown).

It is possible to imagine a mechanism for dimer-mediated helicase unwinding in which the two subunits of the dimer act independently as ATPases. In such a scenario, inhibition of the ATPase reaction by inactive mutant enzymes would not be observed. However, it is considerably more difficult to imagine a dimer-mediated unwinding model in which mutants did not inhibit unwinding of duplex DNA requiring multiple turnovers of the enzyme.

Helicase inhibition assays similar to the ATPase inhibition assays described above were performed, in which the unwinding activity of UvrD was measured in the presence of the same

catalytically compromised mutant enzymes. Mutant enzymes were present at a 3-fold molar excess over wild-type enzyme (higher concentrations of the mutant proteins could not be achieved for technical reasons), and a 20-bp partial duplex DNA substrate was present at a molar concentration slightly greater than the total concentration of enzyme monomers. The step size for UvrD-catalyzed DNA unwinding was recently reported to be 4–5 nucleotides (20). Therefore, displacement of the 20-mer oligonucleotide should require 4–5 cycles of catalysis. Again, the wild-type and mutant proteins were co-incubated prior to initiation of the reaction (see "Experimental Procedures"). A large molar excess of unlabeled 20-mer was included upon initiation of the reaction with ATP to prevent reannealing of displaced radiolabeled 20-mer molecules. This rendered the reactions pseudo-single turnover. Under these conditions, UvrD alone unwound 25% of the DNA substrate (Fig. 6*B*). Unwinding by the three mutant enzymes alone was negligible, as expected. Assuming random association of subunits, a 3:1 ratio of mutant to wild-type enzyme should result in 25% activity compared with wild-type UvrD alone if an active dimeric species were required for unwinding. Fig. 6*B* demonstrates that this result was not obtained. These results, coupled with the ATPase results, indicate that UvrD is functional as a monomer and that oligomerization is not obligatory for catalytic competency.

Although the mutant enzymes could be defective at dimerization, it is unlikely that three separate point mutations in different regions of the protein would all impact oligomerization. However, to ensure that this was not the case, the apparent molecular mass of the three mutant enzymes was determined by gel filtration and compared with UvrD (see Table II). All four proteins exhibited similar apparent molecular masses that were suggestive of a rapid equilibrium between monomeric and oligomeric species. In addition, the UvrD-K35M protein was analyzed by sedimentation equilibrium ultracentrifugation, and the data were described by a monomer ↔ dimer equilibrium with a dissociation constant similar to that of UvrD (data not shown). The average apparent molecular mass for UvrD-K35M was 116.7 kDa, similar to the wild-type value. These results suggest that the oligomerization properties of the mutant enzymes were not compromised.

Non-functional Mutant UvrD Alleles Are Recessive to Wild-type UvrD in Two DNA Repair Pathways—Data obtained from previous genetic studies are also consistent with the conclusion that UvrD is active as a monomer. Site-directed mutagenesis of highly conserved residues in the consensus helicase motifs resulted in the generation of point mutants that failed to function *in vivo* (21, 23, 24, 37, 45). Although previously reported for several UvrD mutants, little attention was directed to the recessive nature of all non-functional alleles in a wild-type *uvrD* background. Table III shows previously published genetic complementation data for four *uvrD* alleles that lack *in vivo* mismatch repair function. When expressed in JH137Δ*uvrD*, none of the mutant alleles substituted for wild-type UvrD (first data column). Furthermore, in JH137, containing a wild-type *uvrD* allele on the chromosome, none of the mutant alleles affected the spontaneous mutant frequency (second column) indicating that the mutant alleles were recessive to the wild-type gene. It should be noted that mutant alleles were expressed at near chromosomal levels as evidenced by Western blots (data not shown). The lack of a dominant negative phenotype is consistent with a model in which UvrD acts as a monomer since the inactive mutant enzymes did not interfere with function of the wild-type enzyme. Similar results were obtained with various other *uvrD* alleles examined for mismatch and/or excision repair function (data not shown). Efforts to overexpress mutant *uvrD* alleles in a wild-type background to observe a dominant negative phenotype were not interpretable since overexpression of wild-type UvrD resulted in UV sensitivity and increased mutation rate.

TABLE III
Genetic complementation experiments

An expression plasmid encoding the indicated allele was transformed into either JH137Δ*uvrD* or JH137. Spontaneous mutant frequency was measured as described (37). Expression of mutant alleles was confirmed by Western blot and was approximately equal to chromosomal expression of the wild-type allele. Relative mutant frequencies with respect to the parental strain, JH137, were obtained by dividing the mutant frequency of each strain by that of JH137. ND, not determined.

Allele	Relative mutant frequency (in JH137Δ*uvrD*)	Relative mutant frequency (in JH137)
uvrD	1.01	ND
uvrDΔ40C	0.92	ND
uvrD-K35M	190	0.67
uvrD-E221Q	62	0.80
uvrD-D220NE221Q	149	0.65
uvrD-Q251E	203	0.70

DISCUSSION

The precise mechanism by which a DNA helicase catalyzes the unwinding of duplex DNA is not known, although it is clear that this process requires energy supplied by the hydrolysis of NTPs. Thus, there must be a coupling of ATP hydrolysis with disruption of the hydrogen bonds between the two strands of duplex DNA. It has been postulated that helicase-catalyzed unwinding requires an oligomeric enzyme (at least a dimer), and reasonably detailed models have been proposed for unwinding by a dimeric (15) or hexameric helicase (5, 46). A fundamental component of these models is the notion that each protomer in the oligomer contributes a DNA-binding site. Thus, an oligomer has at least two DNA-binding sites allowing the enzyme to remain in contact with the DNA, through one of these binding sites, during multiple cycles of unwinding and translocation through a duplex region of DNA.

The dimeric Rep protein and the hexameric T7 gene 4 helicase have been most rigorously studied and currently provide paradigms for an understanding of helicase-catalyzed unwinding. The T7 gene 4 helicase is thought to encircle the ssDNA molecule along which it translocates and utilizes alternate protomers of the hexamer to unwind the duplex region (46). The dimeric Rep protein has been proposed to unwind duplex DNA via a mechanism in which the two protomers alternate binding to ssDNA and dsDNA at the ssDNA/dsDNA junction during cycles of nucleotide binding, hydrolysis, and product release (15). This mechanism is termed the "rolling mechanism" since one can envision the helicase subunits rolling through the duplex region.

Since Rep protein and UvrD share approximately 40% amino acid identity and several biochemical properties, it has been suggested that the two proteins are likely to unwind duplex DNA by the same mechanism involving a dimeric helicase (20). However, we have presented compelling evidence in this report to indicate that the monomeric form of UvrD is an active helicase both *in vitro* and *in vivo*. Therefore, an unwinding mechanism involving a monomeric helicase must be considered, and it is likely that Rep and UvrD unwind DNA by substantially different mechanisms.

The assembly state of active UvrD has been a matter of speculation for some time. Previous studies using gel filtration and protein-protein cross-linking (19) provided evidence to suggest that UvrD forms dimers and higher order oligomers. Protein-protein cross-linking can detect very weak or transient interactions. However, interactions observed with this tech-

nique need to be confirmed with other methods because they may not reflect true association (47). Therefore, we used other reliable physical techniques to investigate the assembly state of UvrD. Gel filtration studies clearly suggest the existence of a population of UvrD monomers and oligomers (presumably dimers) in equilibrium. In addition, analytical equilibrium ultracentrifugation studies using purified UvrD indicate that the enzyme can form dimers with a K_d for dimerization of 3.4 μM. This is the first report of a dissociation constant for the dimerization of UvrD. Interestingly, ATP and/or ssDNA ligands did not enhance the dimerization of UvrD as has been reported for other helicases such as Rep (13, 14) and the phage T7 gene 4 protein (8). In fact, sedimentation velocity ultracentrifugation and gel filtration chromatography experiments suggest that ATP and ssDNA stabilize the monomeric form of UvrD. It is important to note that the dimerization constant reported here is fairly high in relation to the concentration of UvrD present in the cell (0.3–0.8 μM (21)). Therefore, oligomerization of the protein may not be relevant under normal growth conditions (see below), although the possibility of non-ideal behavior *in vivo* resulting in a lower apparent dimerization constant cannot be rigorously excluded.

By using the yeast two-hybrid system we identified a UvrD mutant lacking the C-terminal 40 amino acids that potentially possessed a dimerization defect. Equilibrium ultracentrifugation and gel filtration chromatography confirmed that purified UvrDΔ40C was not able to dimerize *in vitro* in the absence of ligands. Similar to results obtained with wild-type UvrD, ATP, and/or ssDNA did not induce dimerization of UvrDΔ40C. However, this protein maintained full biochemical activity as a helicase and a ssDNA-stimulated ATPase and was fully functional *in vivo* in DNA repair. The simplest interpretation of these results is that UvrDΔ40C is an active monomeric helicase.

The biophysical data clearly indicate that UvrDΔ40C exists as a monomer in solution and, whereas UvrD is capable of dimerization, it too exists as a monomer at protein concentrations typically used for *in vitro* enzymatic assays. Additional biochemical experiments using wild-type UvrD yielded results that were also consistent with a monomeric helicase. The ATPase and helicase activities of UvrD were not significantly inhibited by the presence of a molar excess of ATPase and helicase-deficient UvrD point mutants. Inhibition in these experiments would be expected if dimers or oligomers were required for activity but not if monomers were sufficient for activity. A previous study (21) reported inhibition of UvrD-catalyzed unwinding by the UvrD-K35M mutant. This result was likely due to limiting concentrations of DNA which resulted in competition between wild-type and mutant monomers for the substrate molecules. Based on all the biophysical and biochemical data obtained in this study, we conclude that dimerization of UvrD (or UvrDΔ40C) is not required for activity as a ssDNA-stimulated ATPase nor is it required for helicase activity.

We also note that genetic studies shown here, and reported previously, are consistent with the notion that UvrD is active as a monomer. UvrDΔ40C was fully functional *in vivo,* and since the helicase activity of UvrD has been shown to be required for activity in mismatch and excision repair (21, 23, 24, 37), monomeric UvrDΔ40C (and, by inference, monomeric UvrD) must be active as a helicase in both repair pathways. In addition, a variety of *uvrD* alleles that failed to function in these DNA repair pathways was recessive to wild-type *uvrD* (21, 23, 45). The recessive nature of the mutant *uvrD* alleles examined here suggests that the UvrD helicase activity required in UV excision and methyl-directed mismatch repair does not involve oligomerization. In similar studies, a dominant phenotype has been demonstrated for mutants of the herpes simplex virus type 1 UL9 helicase (48), a protein that is believed to function as a dimer (49, 50).

Taken together, the studies reported here strongly support the conclusion that the active species of UvrD is a monomer and that oligomerization of the protein is either irrelevant or important only when the cellular concentration of UvrD is very high (*e.g.* after SOS induction as discussed below). In fact, these results provide the first direct evidence for a helicase that is able to catalyze duplex nucleic acid unwinding as a monomer. Previous studies using the HCV RNA helicase (51) and purified RecB protein (52) have suggested these enzymes may be functional monomers. It is important to note that the three helicase crystal structures available are all monomers (53–55), although it was argued that the dimeric form of Rep helicase may be resistant to attempts at crystallization. Thus, it is likely that several monomeric helicases exist. Therefore, a mechanism for unwinding by a monomeric helicase must be considered.

Unfortunately, there is not enough mechanistic data available for helicase II to provide a detailed description of its unwinding mechanism. One possible model is based on multiple DNA-binding sites within the monomeric enzyme. This would allow for continuous translocation of the helicase along ssDNA and through dsDNA since at least one binding site would be in contact with the DNA lattice at all times. Processive translocation, made possible by the multiple DNA-binding sites, would likely be driven by conformational changes in the enzyme triggered by nucleotide binding and hydrolysis that are coupled to the actual unwinding event. There is evidence both for helicase II translocation along ssDNA (56, 57) and conformational changes associated with ligand binding (24, 58), lending support to this type of model. In addition, based on the crystal structure of the Rep helicase complexed to ssDNA (54) and site-directed mutagenesis studies of helicase II (24, 41),[2] it is likely that ssDNA is contacted by several distinct regions of the enzyme. Such a model would be fundamentally similar to the "inchworm" model originally proposed for *E. coli* Rep helicase (59, 60). Although less likely, an entirely different type of model is possible for a monomeric helicase in which the helicase does not actively translocate along the DNA molecule. In this model, the enzyme preferentially binds to a ssDNA/dsDNA junction. After each unwinding event, a new junction is made available for another helicase molecule to bind.

If we assume that UvrD translocates along ssDNA during an unwinding reaction, as previous studies have indicated (56, 57) and as suggested by the pseudo-single turnover helicase assays performed here, then a version of the inchworm model for DNA unwinding may be a suitable working model for helicase II-catalyzed unwinding (Fig. 7). This model assumes at least two non-equivalent DNA-binding sites on the monomeric protein. The leading site (*L*) must have an affinity for duplex DNA and may also bind ssDNA, whereas the trailing DNA-binding site (*T*) need only have an affinity for ssDNA. The binding of ATP, its subsequent hydrolysis, and product release would cause the protein to cycle between two or more conformational states as the protein "inches" along the DNA. A cycle of unwinding begins with the enzyme in an "extended" conformation (Fig. 7*A*), in which the *T* site is bound to ssDNA and the *L* site is extended forward in the vicinity of the ssDNA/dsDNA junction. Binding of ATP to the enzyme triggers tight binding of the *L* site to the ssDNA/dsDNA junction and induces a conformational change in the protein to a more compact state in which the *T* site is shifted forward along the DNA lattice with respect to the *L* site (Fig. 7*B*). This results in a transient high affinity DNA binding state. In support of this idea sedimentation ve-

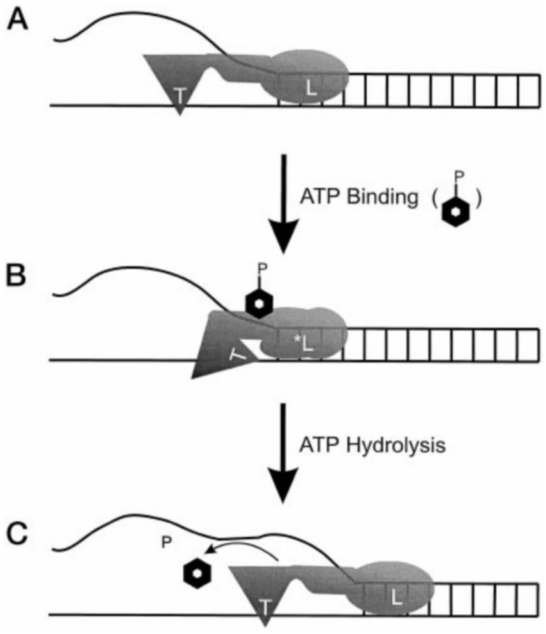

FIG. 7. **Model for duplex DNA unwinding by a monomeric helicase.** A hypothetical model based on available data was generated to describe the mechanism of duplex DNA unwinding catalyzed by the monomeric UvrD helicase. Details of the mechanism are described in the text. The shapes of the helicase and the locations of DNA and ATP-binding sites are arbitrary.

locity ultracentrifugation experiments reported here have shown that the ATP-bound conformational state is more compact than the ATP-free state. In addition, a previous report demonstrated that the ATP-bound state possesses a higher affinity for DNA (24). Upon ATP hydrolysis, a distinct number of base pairs (4–5 according to a recent report (20)) are disrupted at the ssDNA/dsDNA junction, and product release is associated with a return of the enzyme to its original conformation by extension of the *L* site forward with respect to the *T* site (Fig. 7*C*). At this point, the *L* site is in close proximity to the new ssDNA/dsDNA junction, and the cycle is repeated to catalyze further unwinding.

Precedent for the large conformational changes required to fulfill such a model can be seen in the crystal structure of Rep helicase bound to ssDNA (54). The crystal structure of Rep revealed two distinct conformations differing by a 130° rotation of one of the four subdomains with respect to the other three subdomains. The two conformations were referred to as "open" and "closed" because in one orientation the rotating subdomain was extended away from the protein core and in the other orientation it was folded over the bound ssDNA molecule. Since UvrD and Rep share nearly 40% identity at the amino acid sequence level, it is likely that the two proteins adopt similar structures. Indeed, Rep and the PcrA protein from *Bacillus stearothermophilus* also share 40% identity and have crystal structures that are nearly identical (53, 54). Thus, UvrD may be capable of adopting open and closed conformations, similar to those adopted by Rep, that are relevant to its duplex DNA unwinding mechanism. However, it must be noted that the unwinding mechanisms used by UvrD and Rep are likely to be distinctly different.

What is the biological significance, if any, of the dimerization of helicase II? Genetic studies have indicated that a monomer-catalyzed unwinding reaction is sufficient for the role of UvrD in both excision repair and methyl-directed mismatch repair. However, UvrD does oligomerize at high concentration, and helicase II has been observed to coat ssDNA generated during an unwinding reaction in electron microscopic studies (61, 62). We consider two possibilities for the role of UvrD dimerization although there may be others. First, oligomerization of UvrD may play a role in the SOS response in *E. coli*. Under normal growth conditions the majority of UvrD present in the cell, assuming a K_d for dimerization of about 3 μM, is likely to be in a monomeric form. However, SOS induction of the *uvrD* gene can raise the UvrD concentration by as much as 6-fold (63). Under these conditions a significant fraction of the UvrD could be present as dimers. Thus, a role for dimeric UvrD in the cell after SOS induction is possible. The role for UvrD as part of the SOS response is not understood at present but may have something to do with recombinational repair of DNA damage. Second, UvrD is known, from a variety of genetic studies, to have a role in recombination. This role has not been well characterized at the molecular level. In fact, contradictory effects on recombination have been observed in genetic analyses of *uvrD* mutant alleles and in biochemical assays with wild-type UvrD. In some cases *uvrD* mutations correlated with a hyper-recombination phenotype, whereas in other cases recombination was decreased (64–67). Purified helicase II inhibited strand exchange catalyzed by RecA protein under certain conditions but stimulated the same reaction under other conditions (68). These contradictory results may suggest that UvrD has more than a single role in recombination. Perhaps UvrD is required to coat ssDNA to accomplish one of its roles in recombination. Significant structural similarity with RecA protein, which self-associates and coats ssDNA to form nucleoprotein filaments, has been observed in the crystal structures of both Rep and PcrA which, for reasons stated above, are likely to be accurate reflections of the structure of UvrD. We have not, as yet, evaluated the well characterized *uvrD* alleles with regard to their effect on recombination in the cell. Additional experiments will be required to appreciate the role of UvrD oligomerization in the cellular function of helicase II.

Acknowledgments—We thank Dr. James W. George, Dr. Stephen C. Kowalczykowski, and Dr. Aziz Sancar for critical reading of this manuscript. We thank Dr. Chris Lombardo and the UNC Macromolecular Interactions Facility for help with analytical ultracentrifugation. We also thank Susan Whitfield for help in the preparation of figures. Svedberg and SEDNTERP software were written by Dr. John Philo at Amgen, and dCdT was written by Dr. W. Stafford.

REFERENCES

1. Abdel-Monem, M., Durwald, H., and Hoffmann-Berling, H. (1976) *Eur. J. Biochem.* **65,** 441–449
2. Abdel-Monem, M., and Hoffmann-Berling, H. (1976) *Eur. J. Biochem.* **65,** 431–440
3. Matson, S. W. (1991) *Prog. Nucleic Acids Res. Mol. Biol.* **40,** 289–326
4. Matson, S. W., George, J. W., and Bean, D. W. (1994) *BioEssays* **16,** 13–22
5. Lohman, T. M., and Bjornson, K. P. (1996) *Annu. Rev. Biochem.* **65,** 169–214
6. Reha-Krantz, L. J., and Hurwitz, J. (1978) *J. Biol. Chem.* **253,** 4043–4050
7. Mastrangelo, I. A., Hough, P. V. C., Wall, J. S., Dodson, M., Dean, F. B., and Hurwitz, J. (1989) *Nature* **338,** 658–662
8. Patel, S. S., and Hingorani, M. M. (1993) *J. Biol. Chem.* **268,** 10668–10675
9. Bujalowski, W., Klonowska, M. M., and Jezewska, M. J. (1994) *J. Biol. Chem.* **269,** 31350–31358
10. Stasiak, A., Tsaneva, I. R., West, S. C., Benson, C. J. B., Yu, X., and Egelman, E. H. (1994) *Proc. Natl. Acad. Sci. U. S. A.* **91,** 7618–7622
11. Dong, F., Gogol, E. P., and von Hippel, P. H. (1995) *J. Biol. Chem.* **270,** 7462–7473
12. Egelman, E. H., Yu, X., Wild, R., Hingorani, M. M., and Patel, S. S. (1995) *Proc. Natl. Acad. Sci. U. S. A.* **92,** 3869–3873
13. Chao, K. L., and Lohman, T. M. (1991) *J. Mol. Biol.* **221,** 1165–1181
14. Wong, I., Chao, K. L., Bujalowski, W., and Lohman, T. M. (1992) *J. Biol. Chem.* **267,** 7596–7610
15. Wong, I., and Lohman, T. M. (1992) *Science* **256,** 350–355
16. Lahue, R. S., Au, K. G., and Modrich, P. (1989) *Science* **245,** 160–164
17. Caron, P. R., Kushner, S. R., and Grossman, L. (1985) *Proc. Natl. Acad. Sci. U. S. A.* **82,** 4925–4929
18. Husain, I., Van-Houten, B., Thomas, D. C., Abdel-Monem, M., and Sancar, A. (1985) *Proc. Natl. Acad. Sci. U. S. A.* **82,** 6774–6778
19. Runyon, G. T., Wong, I., and Lohman, T. M. (1993) *Biochemistry* **32,** 602–612
20. Ali, J. A., and Lohman, T. M. (1997) *Science* **275,** 377–380
21. George, J. W., Brosh, R. M., Jr., and Matson, S. W. (1994) *J. Mol. Biol.* **235,** 424–435
22. Lechner, R. L., and Richardson, C. C. (1983) *J. Biol. Chem.* **258,** 11185–11196
23. Brosh, R. M., Jr., and Matson, S. W. (1995) *J. Bacteriol.* **177,** 5612–5621

24. Hall, M. C., Ozsoy, A. Z., and Matson, S. W. (1998) *J. Mol. Biol.* **277,** 257–271
25. Hall, M. C., Jordan, J. R., and Matson, S. W. (1998) *EMBO J.* **17,** 1535–1541
26. Miller, J. H. (1972) *Experiments in Molecular Genetics*, Cold Spring Harbor Laboratory, Cold Spring Harbor, NY
27. Laue, T. M., Shah, B. D., Ridgeway, T. M., and Pelletier, S. L. (1992) *Analytical Ultracentrifugation in Biochemistry and Polymer Science* (Harding, S. E., Rowe, A. O., and Hatan, J. C., eds) pp. 90–125, Royal Society of Chemistry, Cambridge, UK
28. Johnson, M. L., Correia, J. L., Yphantis, D. A., and Halvorson, H. R. (1981) *Biophys. J.* **36,** 575–588
29. Laue, T. M. (1995) *Methods Enzymol.* **259,** 427–452
30. Philo, J. S. (1994) in *Modern Analytical Ultracentrifugation* (Schuster, T. M., and Laue, T. M., eds) pp. 156–170, Birkhauser Boston, Inc., Cambridge, MA
31. Philo, J. S. (1996) *Biophys. J.* **72,** 435–444
32. Stafford, W. F. I. (1994) in *Modern Analytical Ultracentrifugation* (Laue, T. M., and Schuster, T. M., eds) pp. 119–137, Birkhauser Boston, Inc., Cambridge, MA
33. Van Holde, K. E. (1975) in *The Proteins* (Neurath, H., and Hill, R., eds) 3rd Ed., pp. 226–287, Academic Press, New York
34. Cantor, C. R., and Schimmel, P. R. (1980) in *Biophysical Chemistry* (Vapnek, P. C., ed) pp. 591–642, W. H. Freeman & Co., New York
35. Gekko, K., and Timasheff, S. N. (1981) *Biochemistry* **20,** 4667–4676
36. Cole, J. L. (1996) *Biochemistry* **35,** 15601–15610
37. Hall, M. C., and Matson, S. W. (1997) *J. Biol. Chem.* **272,** 18614–18620
38. Matson, S. W., and Richardson, C. C. (1983) *J. Biol. Chem.* **258,** 14009–14016
39. Kirkwood, J. G. (1954) *J. Polym. Sci.* **12**, 1–14
40. Bloomfield, V., Van Holde, K. E., and Dalton, W. O. (1967) *Biopolymers* **5,** 149–159
41. Brosh, R. M., Jr., and Matson, S. W. (1996) *J. Biol. Chem.* **271,** 25360–25368
42. Wong, I., and Lohman, T. M. (1997) *Biochemistry* **36,** 3115–3125
43. Notarnicola, S. M., and Richardson, C. C. (1993) *J. Biol. Chem.* **268,** 27198–27207
44. Patel, S. S., Hingorani, M. M., and Ng, W. M. (1994) *J. Biol. Chem.* **33,** 7857–7868
45. Brosh, R. M., Jr., and Matson, S. W. (1997) *J. Biol. Chem.* **272,** 572–579
46. Hingorani, M. M., Washington, M. T., and Moore, K. C. (1997) *Proc. Natl. Acad. Sci. U. S. A.* **94,** 5012–5017
47. Phizicky, E. M., and Fields, S. (1995) *Microbiol. Rev.* **59,** 94–123
48. Malik, A. K., and Weller, S. K. (1996) *J. Virol.* **70,** 7859–7866
49. Fierer, D. S., and Challberg, M. D. (1995) *J. Biol. Chem.* **270,** 7330–7334
50. Makhov, A. M., Boehmer, P. E., Lehman, I. R., and Griffith, J. D. (1996) *J. Mol. Biol.* **258,** 789–799
51. Kim, J. L., Morgenstern, K. A., Griffith, J. P., Dwyer, M. D., Thomson, J. A., Murcko, M. A., Lin, C., and Caron, P. R. (1998) *Structure* **6,** 89–100
52. Phillips, R. J., Hickleton, D. C., Boehmer, P. E., and Emmerson, P. T. (1997) *Mol. Gen. Genet.* **254,** 319–329
53. Subramanya, H. S., Bird, L. E., Brannigan, J. A., and Wigley, D. B. (1996) *Nature* **384,** 379–383
54. Korolev, S., Hsieh, J., Gauss, G. H., Lohman, T. M., and Waksman, G. (1997) *Cell* **90,** 635–647
55. Yao, N., Hesson, T., Cable, M., Hong, Z., Kwong, A. D., Le, H. V., and Weber, P. C. (1997) *Nat. Struct. Biol.* **4,** 463–467
56. Matson, S. W. (1986) *J. Biol. Chem.* **261,** 10169–10175
57. Matson, S. W., and George, J. W. (1987) *J. Biol. Chem.* **262,** 2066–2076
58. Chao, K., and Lohman, T. M. (1990) *J. Biol. Chem.* **265,** 1067–1076
59. Yarranton, G. T., and Gefter, M. L. (1979) *Proc. Natl. Acad. Sci. U. S. A.* **76,** 1658–1662
60. Hill, T. L., and Tsuchiya, T. (1981) *Proc. Natl. Acad. Sci. U. S. A.* **78,** 4796–4800
61. Runyon, G. T., Bear, D. G., and Lohman, T. M. (1990) *Proc. Natl. Acad. Sci. U. S. A.* **87,** 6383–6387
62. Wessel, R., Muller, H., and Hoffmann-Berling, H. (1990) *Eur. J. Biochem.* **192,** 695–701
63. Kumura, K., and Sekiguchi, M. (1984) *J. Biol. Chem.* **259,** 1560–1565
64. Arthur, H. M., and Lloyd, R. G. (1980) *Mol. Gen. Genet.* **180,** 185–191
65. Feinstein, S. I., and Low, K. B. (1986) *Genetics* **113,** 13–33
66. Washburn, B. K., and Kushner, S. R. (1993) *J. Bacteriol.* **175,** 341–350
67. Mendonca, V. M., Kaiser-Rogers, K., and Matson, S. W. (1993) *J. Bacteriol.* **175,** 4641–4651
68. Morel, P., Hejna, J. A., Ehrlich, S. D., and Cassuto, E. (1993) *Nucleic Acids Res.* **21,** 3205–3209